Robotic Framework for Iterative and Adaptive Profile Grading of Sand

Louis Hanut*,[1,5], Yurui Du[2], Andrew Vande Moere[3], Renaud Detry[1,2], Herman Bruyninckx[1,4,5]

***Abstract*— This paper studies sand profile grading, a manipulation task to obtain a desired geometric curve in sand. Manipulating sand is challenging because like other amorphous materials, its properties are difficult to estimate and emergent effects such as collapses may occur which both influence the manipulation outcome. To tackle these challenges, humans iterate and adapt their manual actions to the observed material states. In this paper, we propose to replicate this adaptive and iterative approach on a robotic profile grading task. Our results demonstrate that (1) tool insertion adaptation reduces force limit violations during tool-material interactions, (2) grading angle adaptation ensures no undercutting or collisions while allowing for cutting or smoothing the sand profile, and (3) adapting progress speed to task evolution provides a balance between grading precision and execution time. This paper's findings pave the way for generalized and transferable robotic systems manipulating various amorphous materials and automating a larger set of construction tasks and beyond.**

I. INTRODUCTION

In recent years, automation in the construction sector has become essential to address the rising demand while also mitigating the adverse working conditions faced by construction workers. Many associated tasks involve amorphous materials which motivates researching robotic manipulation of amorphous materials [1]. Those are solids such as sand, soil, plaster, or wet concrete, that have a disordered atomic structure (similar to liquid structures) but that hold their shapes (like solids) when submitted to no external force [2].

The robotics community has investigated the automation of various construction applications where amorphous materials are manipulated, ranging from the excavation of soil trenches [3] to wall plastering [4]. This work focuses on sand profile grading which refers to the process of shaping a material surface from an initial distribution P_{init} to a desired one P_{des} [5], as illustrated in Fig. 1.

For all these applications, the material manipulation is challenging because its properties depend on several parameters (that possibly vary in time and space) and are therefore difficult to model. In addition, emergent effects such as collapses may occur during manipulation. These effects are defined as difficult to predict and non-deterministic: for a same manipulation action, the observed emergent effect will not be exactly the same [6]. They also increase the complexity of perception and, therefore, the uncertainty in the robot's belief about the material state.

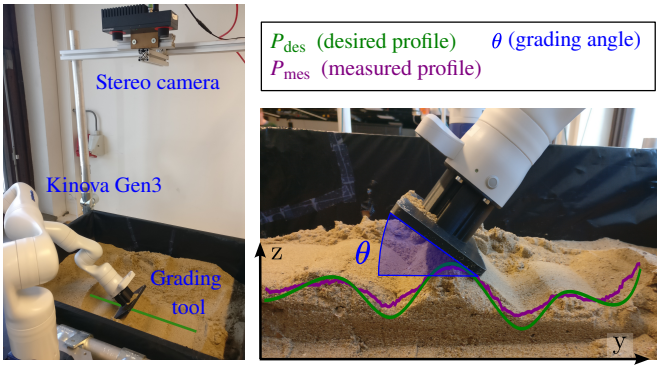

Fig. 1: Experimental setup composed of a 7-DOF-Kinova-Gen3 robotic arm with grading tool, a Roboception rc_visard_160 stereo camera, and a sandbox. Closeup view with the profile grading process definition.

To work with such challenging materials and deal with emergent effects, humans iterate and adapt their manual actions to approach the task objectives progressively, and not in one final go. This paper takes inspiration from human execution and proposes a framework for iterative and adaptive profile grading of sand.

Our methods include adaptation rules to regulate the tool insertion, grading angle and progress speed during an iteration based on interaction feedback with the material of unknown properties.

With this work, our contributions are:

- Development of a framework for iterative sand profile grading including adaptation rules for tool insertion, grading angle, and grading speed.
- Experimental evaluation of the adaptation rules on different profiles and material properties.

II. RELATED WORK

A. Amorphous materials representation

Solid mechanics, discrete element methods, fluid mechanics, or height-map approaches are used for sand modeling [7]. In a dirt cleaning example, a simpler binary map representation was sufficient [8]. The height-map approach is preferred in robotic applications because its moderate computational load allows real-time updates of the material state [9]. In this work, the height-map approach is used to represent the graded profiles.

*Funded by the European Union (robetarme-project.eu). Views and opinions expressed are however those of the author(s) only and do not necessarily reflect those of the European Union or HADEA. Neither the European Union nor the granting authority can be held responsible for them.

* Corresponding author, louis.hanut@kuleuven.be
[1] Department of Mechanical Engineering, KU Leuven, Belgium.
[2] Department of Electrical Engineering, KU Leuven, Belgium.
[3] Department of Architecture, KU Leuven, Belgium.
[4] Department of Mechanical Engineering, TU/e Eindhoven, the Netherlands.
[5] Flanders Make @ KU Leuven, Belgium.

B. Runtime adaptation during robot-material interaction

Multiple solutions have been proposed to adapt to the unknown material properties. A self-tuning impedance controller demonstrated online adaptation to perform scooping actions in diverse amorphous materials [10]. Adaptive excavating iterations allowed to dig desired trenches in various soil while respecting the robot's dynamical limits [3]. This work adopts a similar approach to iteratively shape the profile until the task objectives are met.

C. Human-inspired robot programming

To address the challenging manipulation of amorphous materials, studies have drawn inspiration from human expertise. At the low level, robotic implementations have replicated human-like skills, such as bulldozing primitives [11], [12] or dirt cleaning actions derived from qualitative human observations [8]. Domain knowledge was used to design the action space (smearing, gathering, flipping) and reward function in a Reinforcement Learning (RL) framework [1]. At a higher level, human-inspired heuristics were used to plan sand-shaping actions [13] or to initialize an optimization-based action planner for robotic plastering [4]. Beyond skills and planning algorithms, robots have also been programmed to emulate human workflows. An improved performance was achieved by explicitly structuring a Convolutional Network with distinct scooping and dumping models [14]. Similar to the way humans iteratively plan and validate the outcome of their actions, a robot wiping surfaces used haptic perception to assess performance and refine its action plan [15]. In this paper, the robot uses an iterative workflow analogous to human methods for sand grading, with different adaptation rules inspired by qualitative domain knowledge influencing the grading execution within each iteration.

III. PROFILE GRADING - PROBLEM FORMULATION

The profile grading task illustrated in Fig. 1 is specified with the following objectives, constraints, and simplification assumptions:

Objectives:

- Minimize the profile error, i.e. the distance between the obtained profile distribution P_{mes} and the desired one P_{des}. The profile error metric (PE) is defined as the root mean square error (RMSE) between the measured profile and the desired profile:

$$\text{PE} = \sqrt{\sum_{i=1}^{n} \frac{(z_{i,\text{des}} - z_{i,\text{mes}})^2}{n}}, \tag{1}$$

  where $z_{i,\text{des}}$ and $z_{i,\text{mes}}$ are the desired and measured profile height at pixel i, respectively. n is the number of pixels along the evaluated profile.
- Obtain the specified surface finish properties. In this case, a low surface roughness is desired. The profile roughness metric, Ra, is defined as:

$$Ra = \frac{1}{n} \sum_{i=1}^{n} |z_{i,\text{avg}} - z_{i,\text{mes}}|, \tag{2}$$

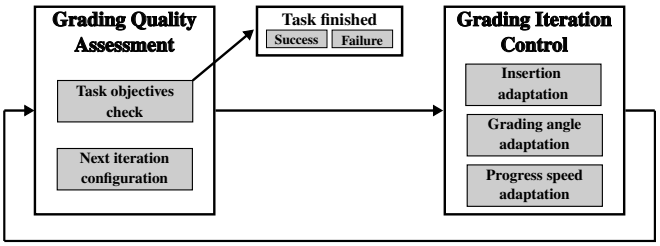

Fig. 2: Iterative profile grading process consisting of two steps: (1) Grading Iteration Control, regulating the robot's motion during an iteration using insertion, angle and speed adaptation rules. (2) Grading Quality Assessment, evaluating the task objectives and configuring the next iteration.

where $z_{i,\text{avg}}$ is obtained by averaging $z_{i,\text{mes}}$ over its neighboring pixels. Therefore, $(z_{i,\text{avg}} - z_{i,\text{mes}})$ corresponds to the high frequency variations of the measured profile only.

Constraints:

- Respect the dynamical limits of the robot.
- The task is asymmetrical: undercutting (i.e., grading deeper than desired profile) should be avoided while overcutting can be compensated by performing an extra iteration.

Simplification assumptions:

Assumption 1: The initial material distribution is higher than, or equal to, the desired one along the whole profile. In that case, the problem is purely subtractive: grading operations are repeated to progressively remove the excess material. The grading trajectory planning is simplified, each iteration covers the whole profile.

Assumption 2: The material is graded along a 1D straight line trajectory.

World Model: The current and desired profiles are stored in the robot's world model. The measured profile is updated in between iterations to avoid occlusions from the robot arm.

IV. METHODS

Fig. 2 illustrates the iterative process employed by the robot during grading of a given profile. This process consists of two essential steps that are repetitively executed until the task is completed. The Grading Iteration Control is responsible for generating the robot's motion during one grading iteration, and it employs multiple adaptation rules to account for material properties and achieve the task objectives while respecting constraints. Following each iteration, the Grading Quality Assessment evaluates the task objectives to determine whether the task is finished, or another iteration is necessary.

A. Grading Iteration Control: Adaptation rules

1) Insertion setpoint adaptation: Since the material properties are not known a priori, the interaction forces during contact can vary significantly and may even exceed the robot's limits [3]. To address this, tool insertion is regulated based on the interaction force between the tool and the material, allowing deviations from the desired profile when

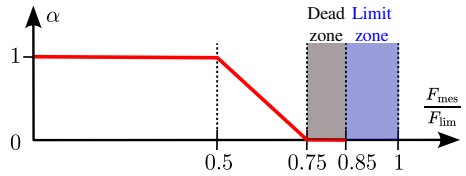

Fig. 3: Definition of α as a function of the measured force F_{mes}. For low forces ($F_{\text{mes}} < F_{\text{lim}}/2$), $\alpha = 1$ such that $z_{\text{setpoint}} = z_{\text{des}}$. For higher forces, α linearly decreases until 0, then $z_{\text{setpoint}} = z_{\text{mes}}$ and the robot maintains its current insertion height. In the dead zone, α is kept at 0. In the limit zone, Equation (4) is overridden and the tool is forced to move away from the material to avoid exceeding the limit.

necessary. The tool insertion is controlled through the vertical velocity v_z using the simple proportional controller defined in (3). The height setpoint z_{setpoint} is determined by the adaptive rule in (4), where α is defined by the empirical mapping shown in Fig. 3. Similar to the self-tuning of the stiffness based on the cartesian position error in the impedance controller in [10], the parameter α adjusts the insertion setpoint based on the measured interaction force. Equation (4) is only valid for $z_{\text{des}} < z_{\text{mes}}$. Otherwise, $z_{\text{setpoint}} = z_{\text{des}}$ to ensure a rapid profile tracking when moving upward and to prevent undercutting.

$$v_z = k\ (z_{\text{setpoint}} - z_{\text{mes}}), \tag{3}$$

$$z_{\text{setpoint}} = z_{\text{mes}} + \alpha\ (z_{\text{des}} - z_{\text{mes}}), \tag{4}$$

2) Grading angle adaptation: The grading angle (θ) adaptation is constrained to avoid undercutting from the front parts of the tool and prevent contacts between the robot links and the material. Additionally, skills-based rules are employed to determine the ideal tool angle based on the desired behavior. For instance, if material needs to be removed, the tool is presented with a higher angle of attack (β, set to 45° arbitrarily), while a smaller angle (parallel to the surface) is used to smooth out the material surface. The implementation is outlined in Algorithm 1, which begins by computing the minimum and maximum possible angles as graphically explained in Fig. 4. Lines 2 to 6 correspond to a behavior switch selecting a cutting or smoothing angle depending on the local distance to the desired profile ($z_{\text{mes}} - z_{\text{des}}$). Finally, the computed angle is constrained to the computed boundaries in line 7.

Algorithm 1 Tool orientation adaptation algorithm. For a given position p_{control}, boundary values are computed to constrain the tool orientation. Based on the distance to the desired profile, a cutting or smoothing angle is adopted.

1: $(\theta_{\text{min}}, \theta_{\text{max}}) \leftarrow$ **Compute_minmax_angle**(p_{control})
2: **if** $(z_{\text{mes}} - z_{\text{des}}) > \Delta z_{\text{threshold}}$ **then**
3: $\quad \theta \leftarrow \beta = 45°$
4: **else**
5: $\quad \theta \leftarrow \theta_{\text{min}}$
6: **end if**
7: $\theta \leftarrow$ **Bound_angle**($\theta_{\text{min}}, \theta_{\text{max}}$)

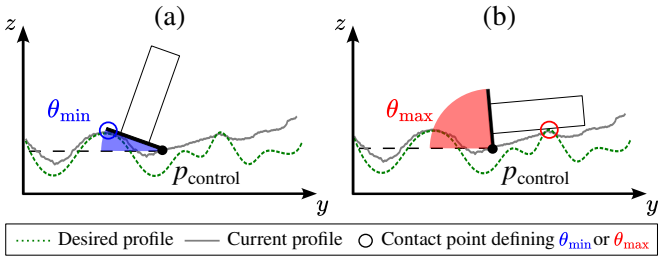

Fig. 4: Orientation adaptation constraints: θ_{min} and θ_{max}. (a) θ_{min} is defined as the minimum angle where the tool does not intersect the desired profile in front of it (avoiding undercutting). (b) θ_{max} is defined as the maximum angle where the robot links do not intersect the material behind p_{control}.

3) Progress speed adaptation: The third adaptation rule controls the speed at which the tool advances along the desired profile. This rule is inspired from the way humans typically work: fast while distant from the objective, and slowing down to achieve greater precision during finishing steps. It is implemented with discrete gain scheduling where the scheduling signal, namely the local profile height error, determines the progress speed values following Table I [16].

TABLE I: Discrete values for the progress speed, determined by the value of the local distance to the desired profile ($z_{\text{mes}} - z_{\text{des}}$).

Scheduling thresholds	$e_{\text{th},1}$	$e_{\text{th},2}$	$e_{\text{th},3}$	$e_{\text{th},4}$
$(z_{\text{mes}} - z_{\text{des}})$ $[mm]$	< 2	$]2;5]$	$]5;10]$	> 10
v_{progress} $[mm/s]$	5	10	20	30

B. Grading Quality Assessment

The Grading Quality Assessment is the process step that takes place between grading iterations. It is responsible to verify the task objectives. The robot terminates its execution if the profile error PE is below a given objective or if the iteration progress (difference between current and previous PE) is smaller than $\Delta\text{PE}_{\text{min}}$. Otherwise, another grading operation is configured. Here, the grading trajectory will always cover the whole profile (considering Assumption 1). In more complex cases, distribution of the material might require more sophisticated iteration configuration.

V. EXPERIMENTS

Two sand profile grading experiments were conducted using the setup shown in Fig. 1. Experiment 1 evaluates the impact of the adaptation rules of Sec. IV-A, and Experiment 2 identifies the framework limitations on more complex profiles. The robot system is composed of a 7-DOF Kinova-Gen3 manipulator arm equipped with a rectangular 3D-printed plastic grading tool (15x10 cm). A Roboception rc_visard_160 stereo camera provides RGB images and depth maps to measure the material surface. The tool-material interaction force is estimated by the internal Kinova controller from the measured joint torques. The robot arm is placed on the side of an 85x66x25 cm box containing ±50 kg of sand. The executed trajectories are centered in the box such that borders have no effects on the obtained profiles.

For both experiments, the sand was manually arranged to have an initial PE of approximately 5.5 cm, ensuring comparable starting conditions and adherence to Assumption 1. The objective PE was set low (2 mm) to observe where the grading process would stop due to insufficient progress ($\Delta \text{PE}_{\text{min}} = 0.5$ mm). The material properties were adjusted by modifying the water content in the sand (wet sand is heavier and more viscous, leading to higher interaction forces with the tool). The moisture level of the sand could take one of the three following values: (S1) dry sand, (S2) dry sand + 0.5 L water, (S3) dry sand + 1.25 L water.

A. Experiment 1: Validation of grading adaptation rules

In this experiment, the tool insertion, angle, and speed adaptation rules were successively evaluated by repeating grading on the profile illustrated in Fig. 7.

1) Results for insertion adaptation: The three profiles obtained (without and with adaptation using $F_{\text{lim}} = 30$ or 50 N) are geometrically similar (as shown in Fig. 7 (a)).

The interaction force between the tool and the material is depicted in Fig. 5 for the non-adaptive case with sand level S2, along with a histogram to better visualize the proportion of measurements that exceed the force threshold. Table II contains the percentage of force violation for the different testing conditions. These results suggest that adapting the tool insertion helps regulating the interaction force for the different sand moisture levels (and therefore material resistance) and with different imposed limits.

Fig. 6 illustrates how the insertion setpoint is adapted based on the measured force, as described in (4). Although the insertion adaptation reduces the force excesses, force peaks are still observed. These peaks occur at profile summits, where the desired angle to follow the curvature, θ_{des}, decreases rapidly. The grading angle adaptation rule does not account for material accumulated in front of the tool, which becomes compacted when θ decreases, resulting in sudden, high reaction forces from the sand. The force peak at the end of the profile is more pronounced due to the increased accumulation of material.

TABLE II: Percentage of measurements that violate force limits in Experiment 1.1. The adaptive versions allow to keep that percentage lower (at least 50% violation reduction).

Configuration	$F_{\text{lim}} = 30$ N		$F_{\text{lim}} = 50$ N	
Insertion Adaptation	On	Off	On	Off
Sand level S2	8.09	18.28	4.96	9.88
Sand level S3	6.86	21.25	4.68	11.29

2) Results for grading angle adaptation: Fig. 7 (b) shows that undercutting occurs when θ is fixed at 10° due to the presence of features in the profile whose tangent is larger than 10°. The tool size impacts the area where undercutting can occur, as indicated in red in Fig. 7 (b). With a low θ, the iterations progress slower because the tool is inserted with a larger contact area which leads to higher interaction forces.

Additionally, we tested the hypothesis that grading with a large tool angle results in rougher surface finish. The surface

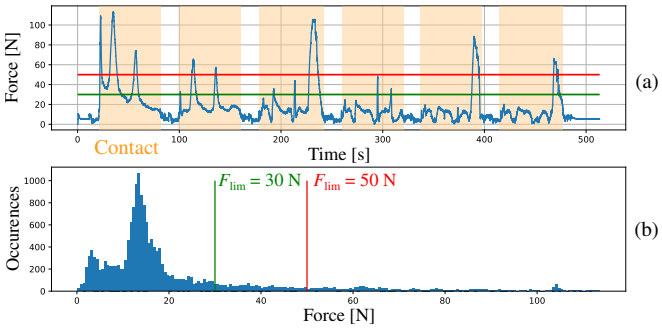

Fig. 5: Estimated force at the end effector for Experiment 1.1 (with sand level S2 and without insertion adaptation). (a) Force measurements over time. (b) Histogram to visualize the proportion of force measurements exceeding the force limit during contact.

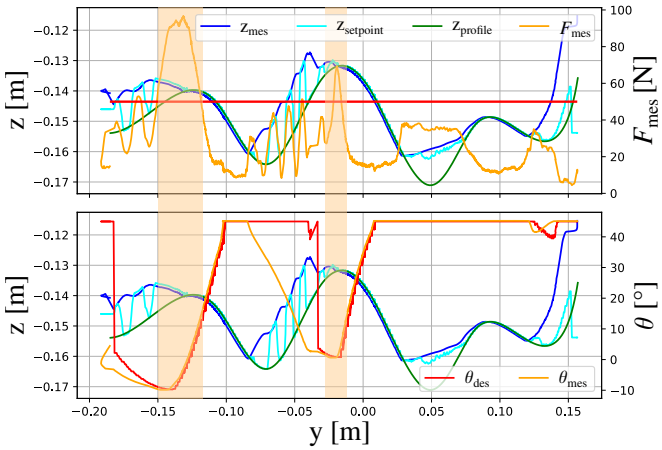

Fig. 6: Measured height, grading angle, and force during an iteration (with insertion adaptation and sand level S2). Orange areas highlight the moments where the measured force suddenly increases. This is due to compaction of the accumulated material while the tool angle changes rapidly (at hill peaks).

roughness obtained with θ fixed at 45° ($Ra_{45} = 0.36$ mm) should be higher than with $\theta = 10°$ ($Ra_{10} = 0.25$ mm) or with angle adaptation ($Ra_{\text{adaptive}} = 0.32$ mm). Although the measured values concur with the hypothesis, those are close to the camera depth resolution (0.4 mm) which suggests that a better roughness estimation method is required for a rigorous hypothesis validation.

3) Results for progress speed adaptation: In Fig. 7 (c), a trade-off can be observed between profile similarity (improved when progress speed is lower) and execution speed. The experiment with the speed fixed at 3 cm/s leads to a spatial shift between the obtained and desired profiles due to delays in the insertion controller. The adaptive approach allows to take advantage of the task progress to switch between rapid grading when the objective is still far and then work with more precision for the finishing steps, as indicated by the results in Table III.

B. Experiment 2: identification of limitations

This Experiment, with sand of moisture level S1 and S2, grades five profiles (Fig. 8(g)) whose shape complexity was expected to require better performance than the presented

TABLE III: Comparison of the obtained PE and the total execution time after third iteration (last iteration for $v = 3$ cm/s).

	$v = 5$ mm/s	$v = 3$ cm/s	Adaptive speed
Obtained PE [mm]	5.03	9.19	5.66
Execution time [s]	254.63	89.93	200.8

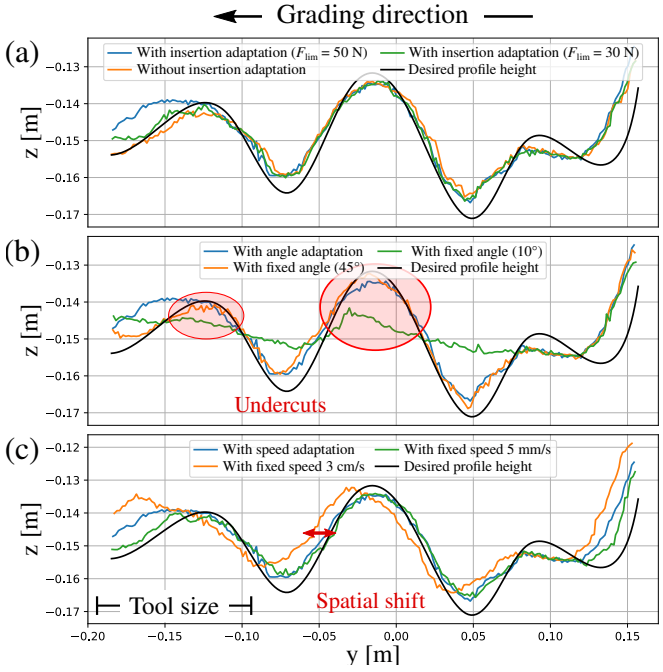

Fig. 7: Profiles obtained after the last iteration in Experiment 1. (a) With and without insertion adaptation: no significant geometric difference is observed. (b) With and without angle adaptation: a low fixed angle (10°) leads to undercutting. (c) With and without speed adaptation: there is a trade-off between profile grading fidelity (with lower speed) and speed execution (with faster grading). The profiles are graded from right to left, the tool size is indicated in (c).

framework can offer. The results are reported in Table IV. All profiles exhibited low force violation percentage for both sand moisture levels, except for profile 3, in which force peaks similar to those observed in Experiment 1 were detected on the last hill. For each profile, the obtained PE is lower with sand S2 than S1, as it is also shown in Fig. 8.

Steeper slopes can be graded in wetter sand due to the increased repose angle, which is influenced by the water content and characterizes the inherent stability of the material [17]. As shown in Fig. 8(c) and (e), the vertical steps could not be obtained in dry sand (S1), resulting in higher PE and even collapses (see green area in (c)). The desired profile is steeper than allowed by the sand natural stability and so it collapsed to form a slope at its repose angle which is graphically computed to a value of 33°, as highlighted in yellow in (c). Wetter sand could be graded more deeply in the valleys, as shown in Fig. 8(b) compared to (a).

In Fig. 8(d) and (f), the steps are not perfectly vertical due to controller limits, specifically the ratio between vertical and horizontal speed (see yellow highlights in (d)). Higher angles could be obtained by increasing the control gains or limits of the vertical speed control rule. Another possibility is to extend the profile specification and add control points along the steep cliffs. On the profile of Fig. 8(f), the arbitrary limit that we imposed for the max angle (60°) is seen on the rising steps.

Finally, an emergent effect appeared while grading valleys deeper. The accumulated material then pushed on the following hill peaks, causing a shift of the hill peak that appears as undercutting. This effect, which we will refer to as Accumulation shift, is observed on profiles 1, 2, and 3 for both S1 and S2 sand, but is more pronounced with S2 as the valleys are deeper (see yellow highlights in Fig. 8(a) and (b)). Due to the negative impact of Accumulation Shift on the progress metric PE, the grading process terminates before completely digging the profile valleys.

VI. DISCUSSION

Experiment 1 demonstrated the effectiveness of the adaptation rules introduced in Sect. IV-A. The grading angle adaptation rule enabled the switching between cutting and smoothing angles based on task progress, avoiding undercutting and collisions between the robot links and material. The progress speed adaptation provided a good balance between profile grading precision and execution time.

Experiment 1.1 shows that the insertion adaptation rules reduced at least 50% of the force limit violations. Those violations can be completely eliminated with a better handling of force peaks resulting from accumulated material compaction. To achieve this, the condition to cut or smooth (line 2 of Algorithm 1) could be refined to use the measured force and adopt the cutting angle when material resistance is high. An adaptation rule that prevents any force limit violation ensures that the grading task can be performed regardless of the robot capabilities and the graded material's resistance. This means that any robot can grade any material (a weaker robot will simply require more iterations to reach the task objectives).

Experiment 2 reveals several limitations of the current grading framework. The material itself imposes constraints, such as the repose angle visible in Fig. 8(c) and (e), and emergent effects like collapses and accumulation shifts. Without actively altering the material properties, the robot can at best monitor its own execution to detect such occurrences and adjust future actions accordingly (e.g., how to satisfyingly adjust the desired profile considering the maximum angle before collapse).

Additionally, the robot, its tool, and control rules restrict the complexity of profiles that can be graded. Specifically, steep cliffs are limited by the control bandwidth and the imposed maximum angle.

In this paper, several parameters (α, β and $e_{\text{th,1-4}}$) were defined arbitrarily. While these parameters could be tuned, adapted, or learned to enhance the manipulation of specific materials, this work deliberately focuses on simple control rules, relying on limited knowledge of material behavior (primarily trends). This approach highlights the trade-off between optimality and versatility, as more sophisticated control rules may yield improved performance in specific

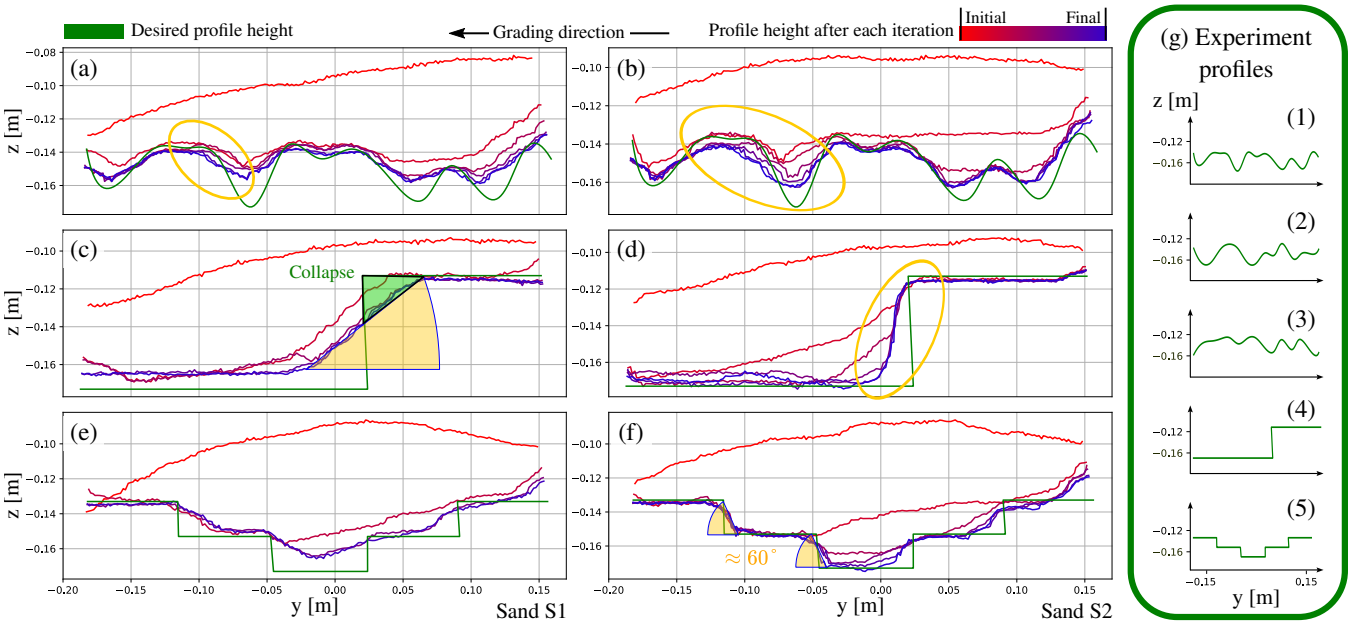

Fig. 8: (a-f) Evolution of the profiles throughout the grading process of sand S1 and S2. Profile 1 is shown in (a) and (b), profile 4 in (c) and (d), and profile 5 in (e) and (f). (g) Profiles used in Experiment 2. Profiles 1, 2 and 3 are obtained from cubic spline interpolation between 15 randomly generated equidistant points. Profile 4 is a step. Profile 5 is a staircase profile (series of falling and rising steps).

TABLE IV: Results for Experiment 2. Each profile from Fig. 8(g) is graded on S1 and S2 sand. The table contains different metrics characterizing the quality of the grading task: (a) the profile error between the measured and desired profile (in mm), (b) the percentage of force limit violations, (c) the maximum force (in N) measured throughout the whole task execution, (d) the observed emergent effects types (C: Collapse, AS: Accumulation shift, /: none), and (e) the number of iterations required before terminating (insufficient progress).

Graded profile	1		2		3		4		5	
Sand moisture level	S1	S2	S1	S2	S1	S2	S1	S2	S1	S2
(a) Profile error [mm]	7.15	5.96	7.4	5.29	8.35	9.59	11.22	10.3	7.98	5.1
(b) Percentage of force violation [%]	0.33	1.28	0.77	0.94	7.15	6.11	1.45	2.06	0.51	1.92
(c) Maximum force measured [N]	56.96	85.4	80.74	84.31	129.09	141.94	81.29	84.33	77.14	74.55
(d) Emergent effects	AS	AS	AS	AS	AS	AS	C	/	/	/
(e) Number of iterations	5	6	6	7	6	4	4	5	3	5

scenarios but may also reduce adaptability to changing conditions.

Future work may involve extending the profile grading task to tackle profiles specified over 2D surfaces, rather than the current linear specification. This will require advanced planning algorithms between iterations to find adequate material redistribution trajectories [4], [8], [13]. Additionally, a better handling of emergent effects could improve task quality, by detecting and identifying the observed emergent effects and their implications on the world model and future actions (e.g., triggering a recovering action in response to emergence or adapting task objectives based on material limits). Finally, the framework could be generalized to more complex applications by improving it to allow for multi-skill tasks, where the assessment step between iterations selects and configures the most adequate skill to perform.

VII. CONCLUSIONS

In this paper, we present a framework for the iterative and adaptive profile grading of sand. The tool insertion adaptation reduces the percentage of force limit violations during tool-material interactions. Additionally, the grading angle adaptation allows to switch between cutting and smoothing behaviors based on task progress, while avoiding undercuts and collisions between sand and robot links. Moreover, adapting the speed to the task progress provides a balance between grading precision and execution time.

However, in cases of large emergence effects, the robot may not be able to resolve the situation, resulting in significant deviations from the desired profile. To address this, the framework can be expanded to include emergence handling mechanisms to recover from emergent situations if possible. Otherwise, emergence monitors can be employed to adapt the world model and robot capabilities for future executions.

We envision the potential for generalizing this approach to other amorphous material manipulation tasks using this iterative process as a framework, where multiple task-specific skills would contain the necessary knowledge-based behaviors to perform iterations, while the inter-iteration component would deal with situation awareness and skill configuration.

REFERENCES

[1] Y. Zhang, W. Yu, C. K. Liu, C. Kemp and G. Turk, "Learning to manipulate amorphous materials", ACM Trans. Graph., vol. 39, no. 6,

2020.
[2] CNRS. "Amorphous Materials: How Some Solids Flow Like Liquids." ScienceDaily. www.sciencedaily.com/releases/2008/07/080704153507.htm
[3] D. Jud, P. Leemann, S. Kerscher and M. Hutter, "Autonomous free-form trenching using a walking excavator", IEEE Robot. Automat. Lett., vol. 4, no. 4, pp. 3208-3215, Oct. 2019.
[4] M. A. Kuhlmann-Jørgensen, J. Pankert, L. L. Pietrasik, and M. Hutter, "PLASTR: Planning for Autonomous Sampling-Based Trowelling," IEEE Robotics and Automation Letters, vol. 8, no. 8, pp. 5069–5076, Aug. 2023, doi: 10.1109/LRA.2023.3291894.
[5] Wikipedia contributors, "Grading (earthworks)," Wikipedia, The Free Encyclopedia, https://en.wikipedia.org/w/index.php?title=Grading_(earthworks)&oldid=1218543573
[6] Tokac, I., Philips, J., Bruyninckx, H. et al. Fabrication grammars: bridging design and robotics to control emergent material expressions. Constr Robot 5, 35–48 (2021). https://doi.org/10.1007/s41693-021-00053-0
[7] W. Kim, C. Pavlov, and A. M. Johnson, "Developing a Simple Model for Sand-Tool Interaction and Autonomously Shaping Sand," arXiv, Aug. 2019. doi: 10.48550/arXiv.1908.02745.
[8] S. Elliott and M. Cakmak, "Robotic Cleaning Through Dirt Rearrangement Planning with Learned Transition Models," in 2018 IEEE International Conference on Robotics and Automation (ICRA), May 2018, pp. 1623–1630. doi: 10.1109/ICRA.2018.8460915.
[9] K. Tsuruta, S. J. Griffioen, J. M. Ibáñez, and R. L. Johns, "Deep Sandscapes: Design Tool for Robotic Sand-Shaping with GAN-Based Heightmap Predictions," in 2022 Annual Modeling and Simulation Conference (ANNSIM), Jul. 2022, pp. 730–741. doi: 10.23919/ANNSIM55834.2022.9859472.
[10] P. Balatti, D. Kanoulas, N. G. Tsagarakis, and A. Ajoudani, "Towards Robot Interaction Autonomy: Explore, Identify, and Interact," in 2019 International Conference on Robotics and Automation (ICRA), May 2019, pp. 9523–9529. doi: 10.1109/ICRA.2019.8794428.
[11] C. Ross, Y. Miron, Y. Goldfracht, and D. D. Castro, "AGPNet - Autonomous Grading Policy Network," ISARC Proceedings, pp. 40–43, May 2022.
[12] Y. Miron, Y. Goldfracht, C. Ross, D. D. Castro, and I. Klein, "Autonomous Dozer Sand Grading Under Localization Uncertainties," IEEE Robotics and Automation Letters, vol. 8, no. 1, pp. 65–72, Jan. 2023, doi: 10.1109/LRA.2022.3222990.
[13] A. Cherubini, V. Ortenzi, A. Cosgun, R. Lee, and P. Corke, "Model-free vision-based shaping of deformable plastic materials," The International Journal of Robotics Research, vol. 39, no. 14, pp. 1739–1759, 2020, doi: 10.1177/0278364920907684.
[14] C. Schenck, J. Tompson, S. Levine, and D. Fox, "Learning Robotic Manipulation of Granular Media," PMLR, Oct. 2017, pp. 239–248. Accessed: Mar. 13, 2023. [Online]. Available: https://proceedings.mlr.press/v78/schenck17a.html
[15] D. Leidner, G. Bartels, W. Bejjani, A. Albu-Schäffer, and M. Beetz, "Cognition-enabled robotic wiping: Representation, planning, execution, and interpretation," Robotics and Autonomous Systems, vol. 114, pp. 199–216, Apr. 2019, doi: 10.1016/j.robot.2018.11.018.
[16] W. J. Rugh and J. S. Shamma, "Research on gain scheduling", Automatica, vol. 36, pp. 1401-1425, 2000.
[17] Nowak, S., Samadani, A. and Kudrolli, A. Maximum angle of stability of a wet granular pile. Nature Phys 1, 50–52 (2005). https://doi.org/10.1038/nphys106